Supplementary information for

An efficient chitosan/silica composite core-shell microspheres supported Pd catalyst for aryl iodides Sonogashira coupling reactions

Qing Cui [a, b], *Hong Zhao* [a], *Guangsheng Luo* [a], *Jianhong Xu* [a*]

[a] The State Key Lab of Chemical Engineering, Department of Chemical Engineering, Tsinghua University, Beijing 100084, China. [b] School of Chemistry and Chemical Engineering, Shandong University, Jinan 250100, China. [*] Corresponding author. Email: xujianhong@tsinghua.edu.cn

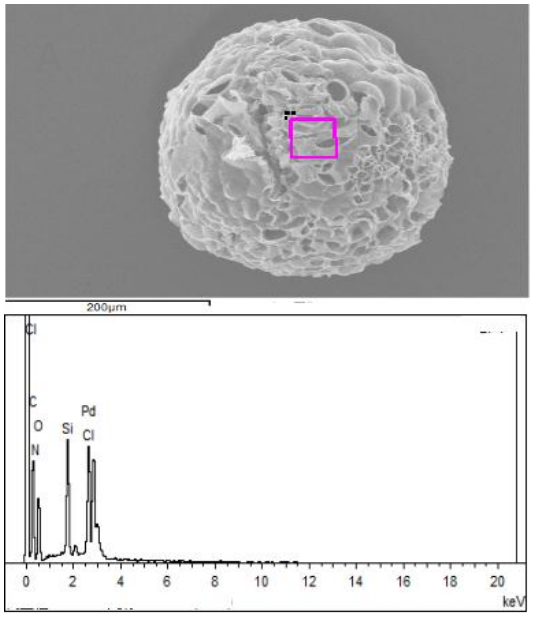

Figure S1. SEM and EDS analysis of chitosan/silica core-shell microspheres.

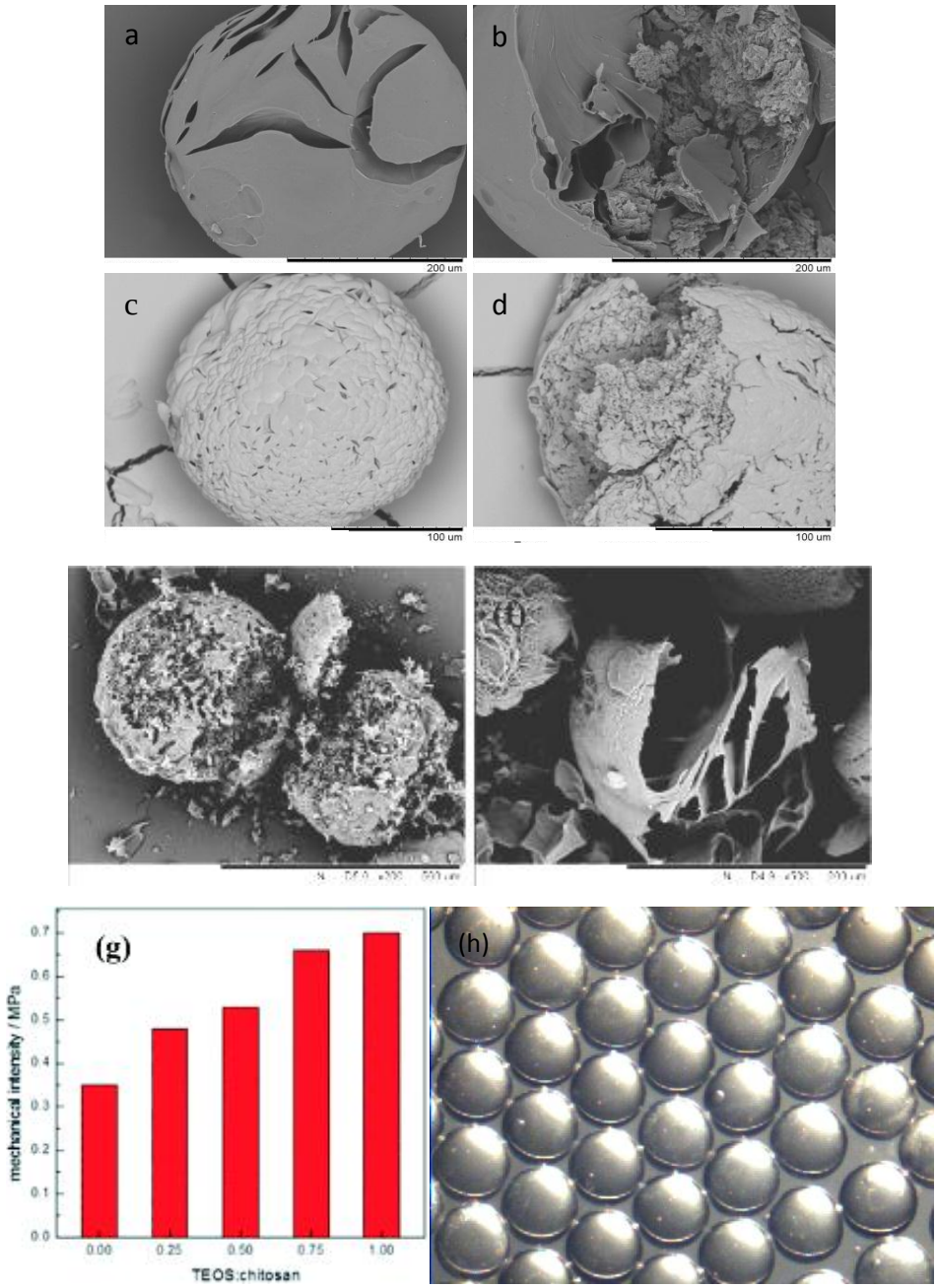

Figure S2. Morphology of microspheres processed by different curing time.
(a)(b) SEM images of surface and interior of microspheres whose curing time is too short. The external pores were shaped gully, while internal ones were huge and few. **(c)(d)** SEM images of microspheres whose curing time is too long. Surface and interior of microspheres both gradually began to densify, and pores rarely left. (e)(f) SEM images of microspheres with uniform component and microspheres with core–shell structures, respectively, after calcination.[1] (g) mechanical properties of the hybrid microspheres with different chitosan/silica ratios.[1](h) microscopic image of uniform microspheres prepared by using the microfluidic device.

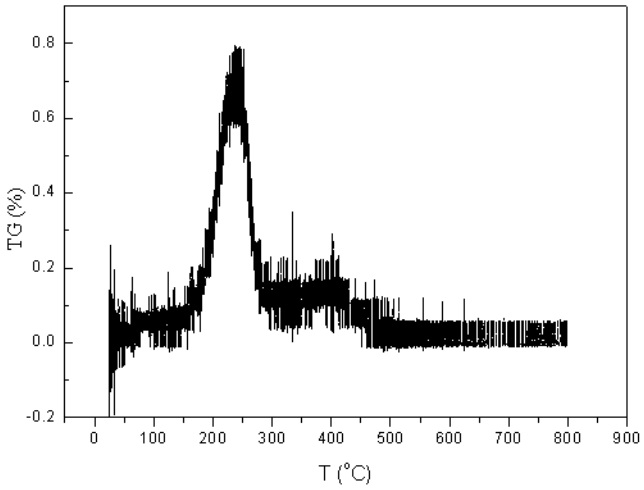

Figure S3. Thermogravimetric analysis of chitosan/silica microspheres.

Table S1. Detail of the equilibrium adsorption data

Conc. before the adsorption (ppm)	Conc. After the adsorption (ppm)	Adsorption conc. (ppm)	Amount of microspheres (g)	Amount of ultrapure water (g)	Equilibrium absorption capacity (mg/g)	Loading capacity (%)
10.92	0.612	10.308	0.02	60	30.93	3.093
21.67	1.611	20.059	0.02	60	60.186	6.018
29.04	6.106	22.934	0.02	60	68.81	6.881
32.6	2.653	29.947	0.02	50	74.87	7.487
39.08	14.081	24.999	0.02	60	75.019	7.502
45.98	9.933	36.047	0.02	50	103.006	10.300

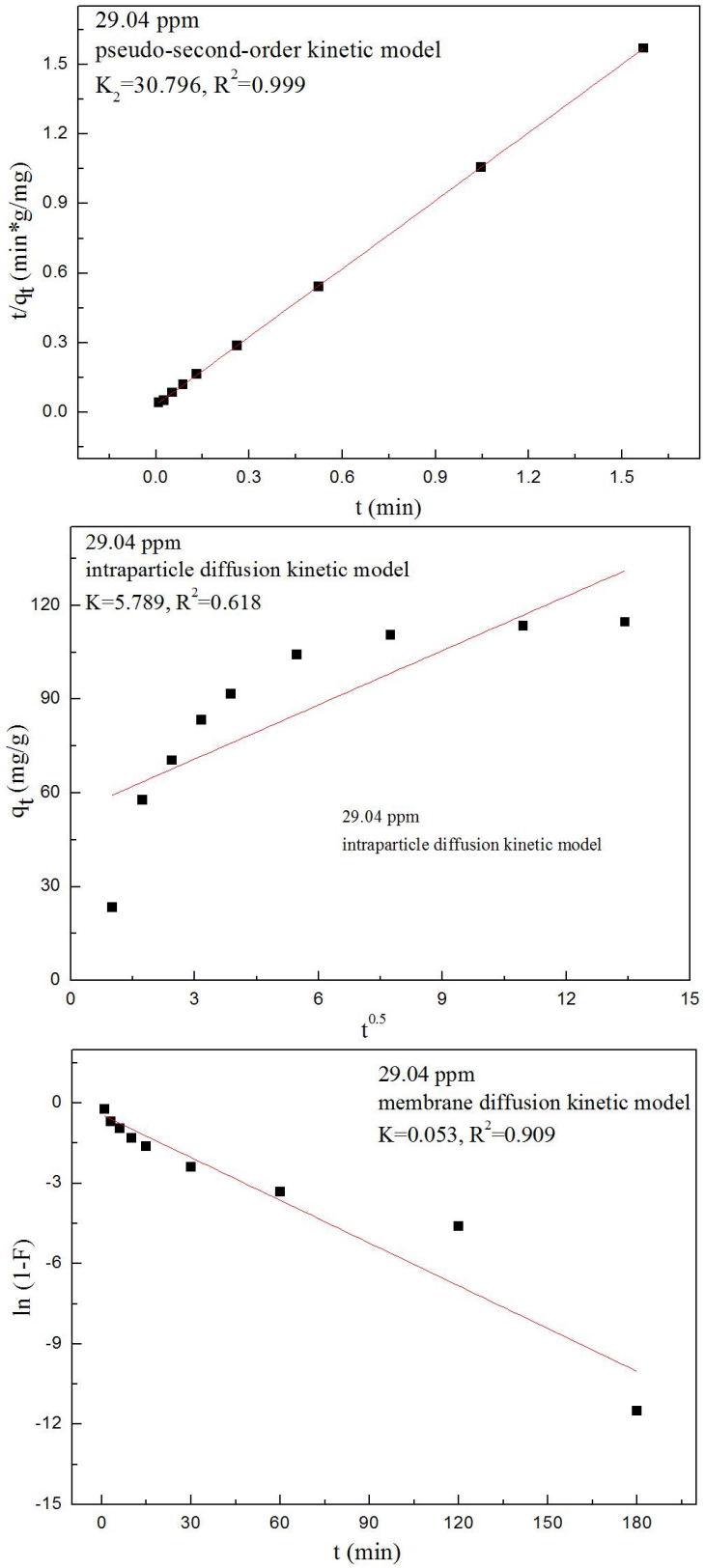

Figure S4. kinetic data from where initial Pd (II) concentration is 29.04 ppm.

Protocol 1:

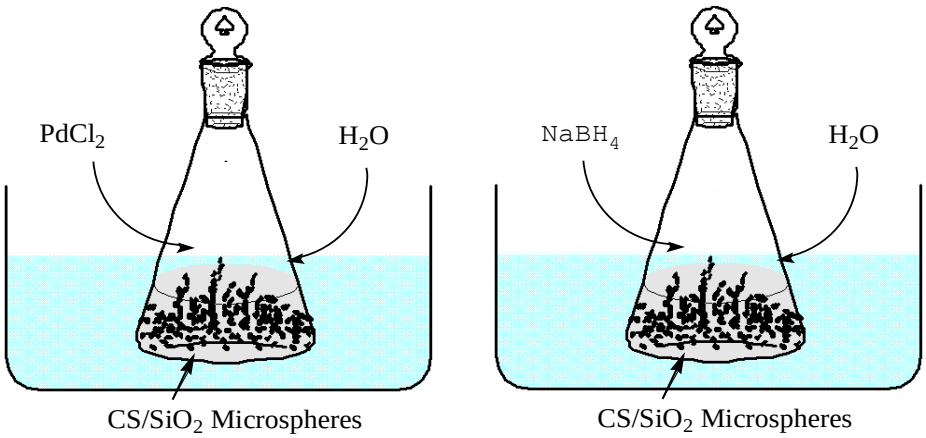

Protocol 2:

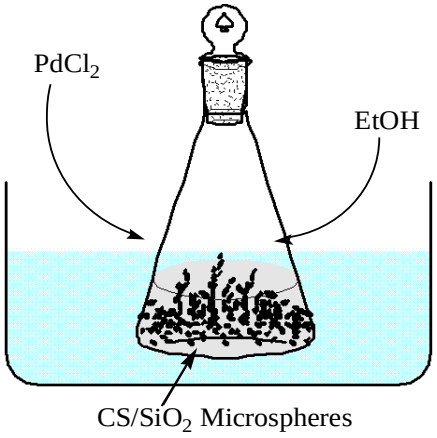

Protocol 3:

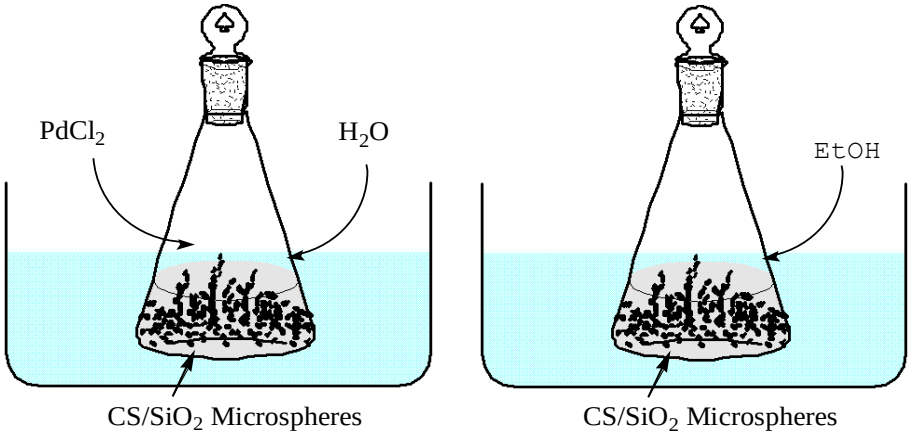

Figure S5. Detailed procedure of three Palladium loading patterns. The entire loading processes were completed in a shaking water bath, 25℃, and had a fixed adsorption time.

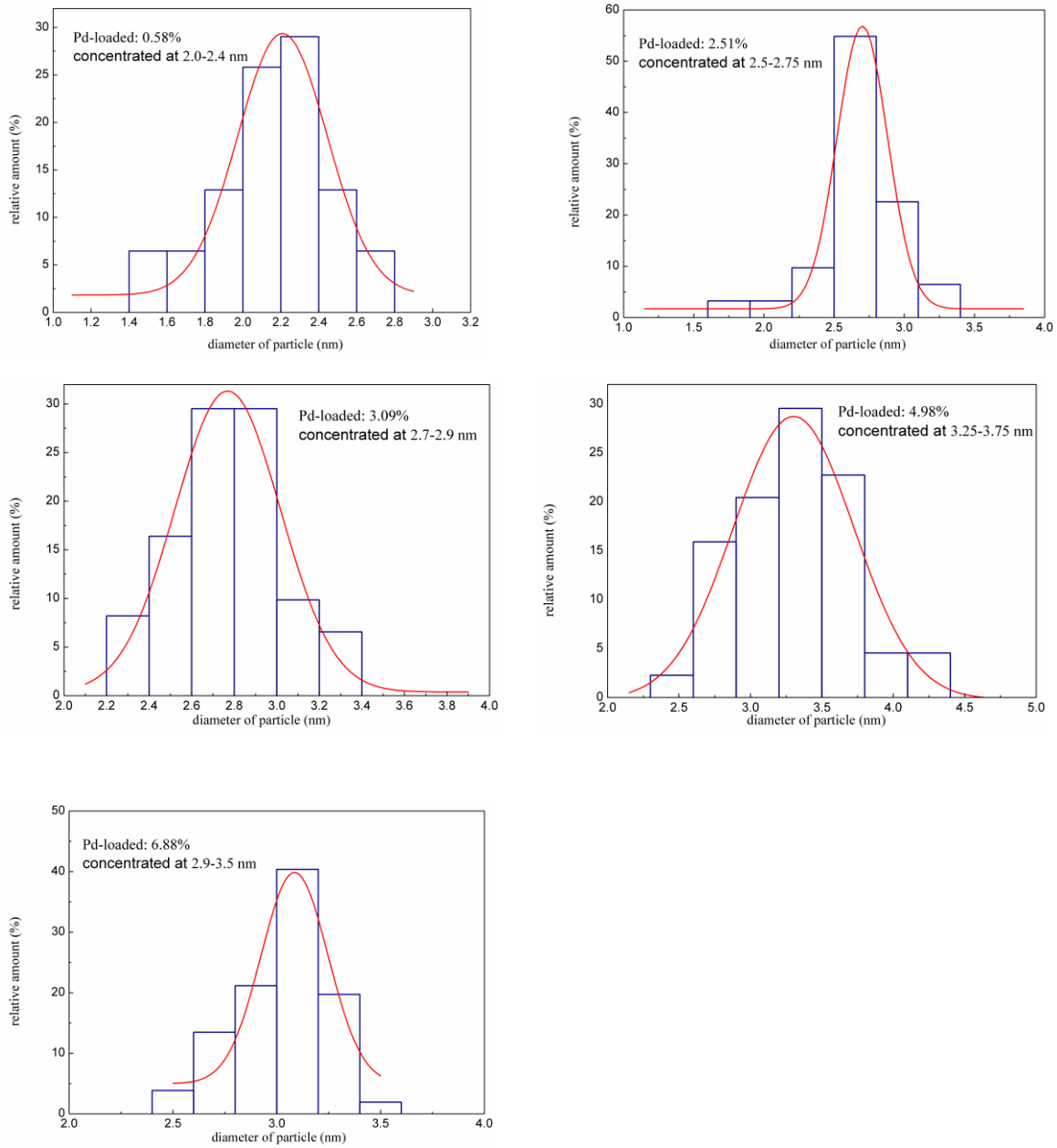

Figure S6. Particle size distribution under different Pd-loaded capacity (Pattern 1). Microspheres loading Pd from 0.58 wt.% to 6.88 wt.% are all pretty uniform, and their particle size distribution is relatively narrow.

Table S2. Optimization of the reaction conditions. Amount of catalyst, reaction time and amount of loaded Palladium were studied

Amount of catalyst:10 mg	**Time:6 h**		
Palladium loaded	1%	3%	5%
Yield	98.7%	98.9%	99.82%
Space-time Yield g/(g*h)	7.238	7.253	7.320
Amount of catalyst:10 mg	**Palladium loaded:1 wt.%**		
Time	4h	5h	6h
Yield [a]	87.25%	99.2%	98.7%
Space-time Yield g/(g*h) [b]	9.5975	8.7296	7.238
Palladium loaded:1 wt.%	**Time:6 h**		
Amount of catalyst	2mg	5mg	10mg
Yield	86.66%	98.9%	99.2%
Space-time Yield g/(g*h)	38.1304	17.4064	8.7296

[a] Isolated yield. [b] Space-time Yield(STY) is the weight of product obtained per gram of supported catalyst in one hour.

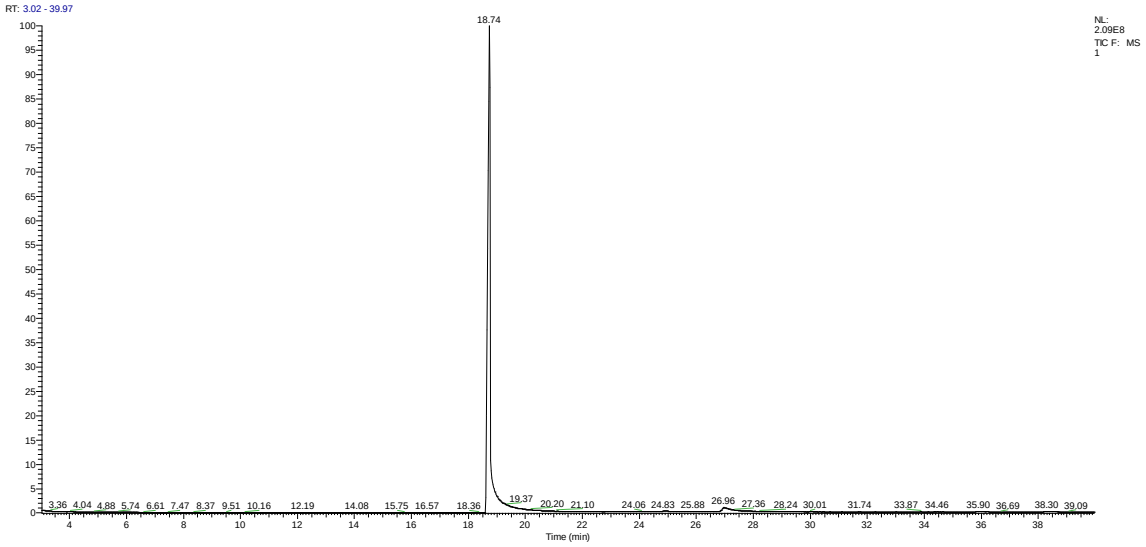

Apex RT	Start RT	End RT	Area	%Area	Height	%Height
18.74	18.45	20.28	1542775641	96.1	208597774.7	98.81
24.83	24.69	25.5	5510975.913	0.34	297590.539	0.14
26.96	26.69	28.57	51120687.03	3.18	1741009.787	0.82
35.9	35.73	36.04	1969289.615	0.12	213619.447	0.1
38.3	38.09	38.67	3965467.532	0.25	266769.789	0.13

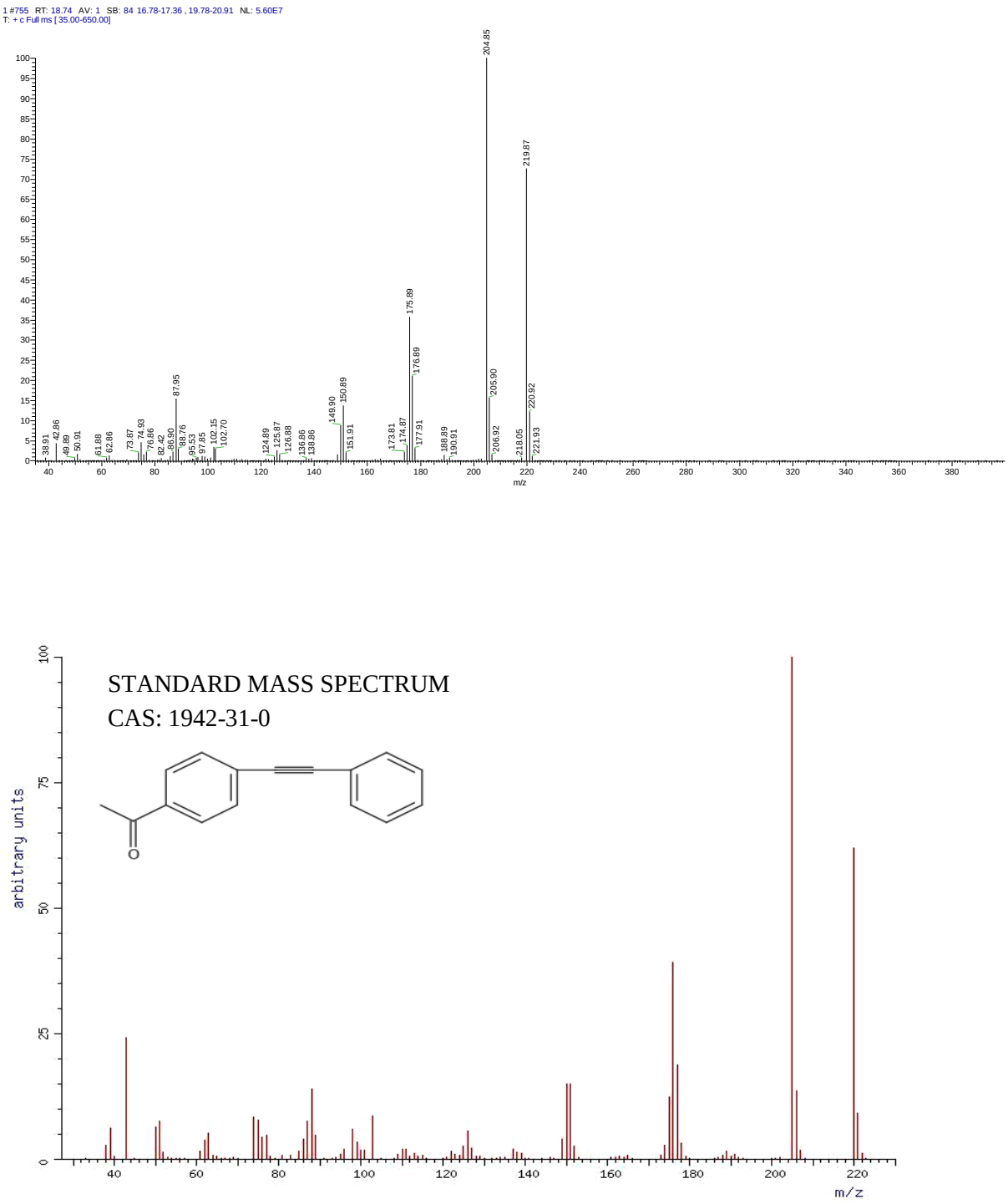

Figure S7. Mass spectrum of the product of Sonogashira coupling reaction between 4-iodoacetophenone and phenylacetylene.

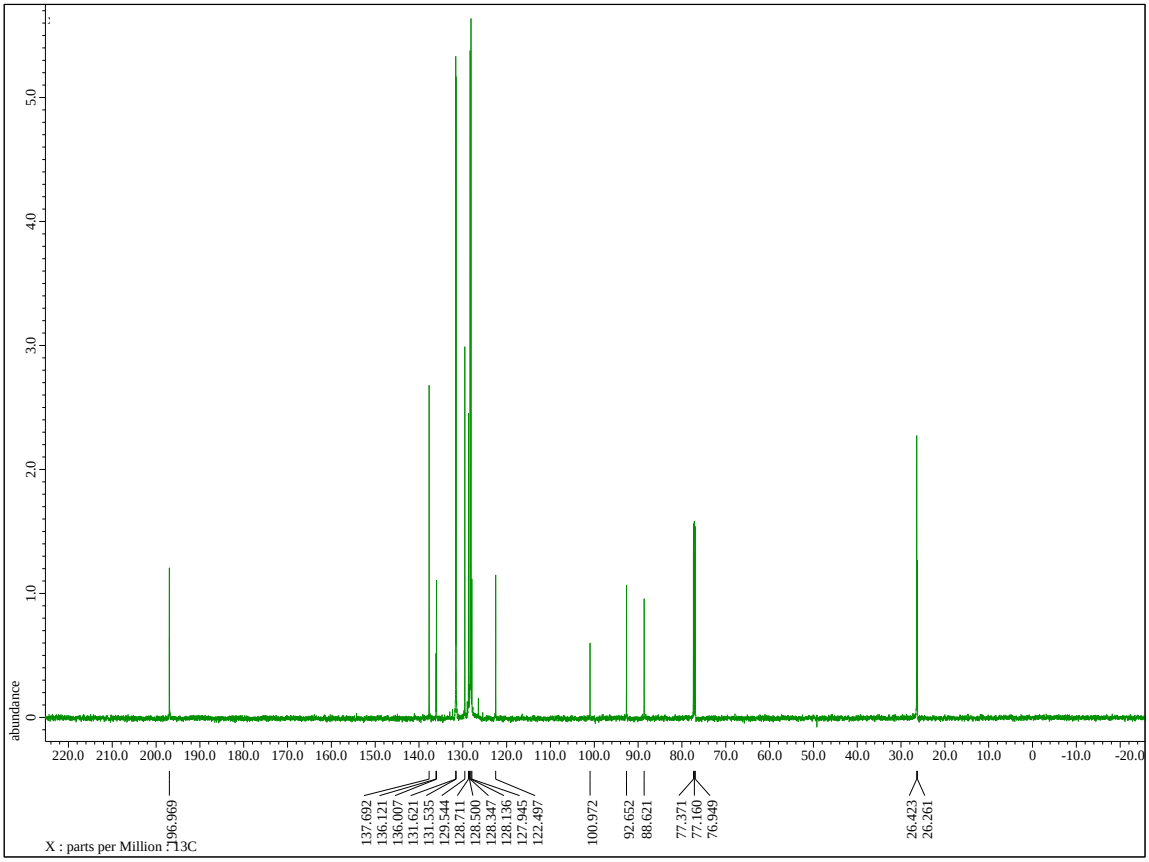

Figure S8. ^{13}C NMR spectrum of the product of Sonogashira coupling reaction between 4-iodoacetophenone and phenylacetylene.

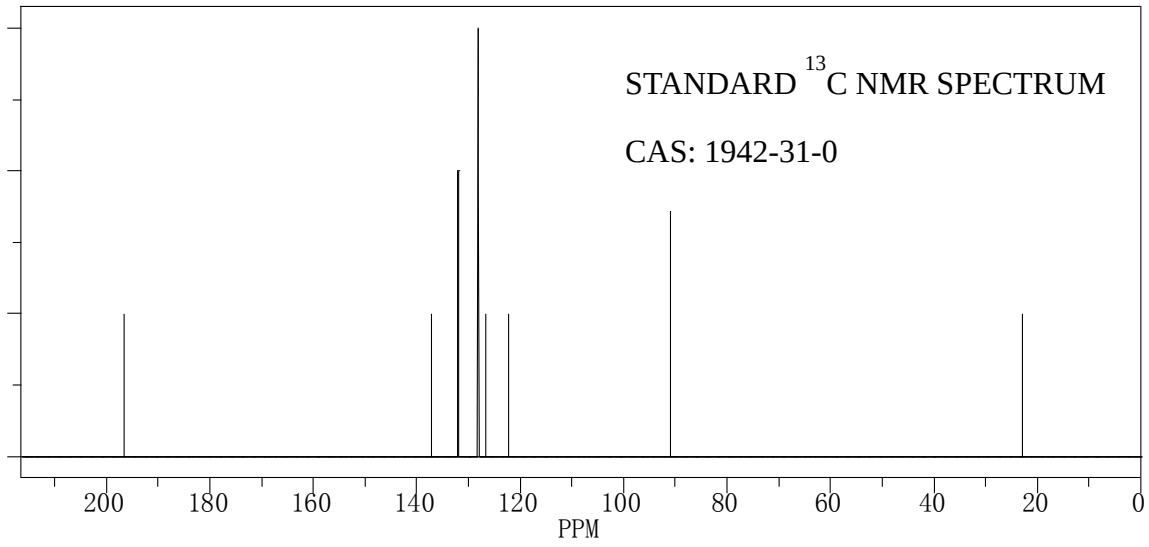

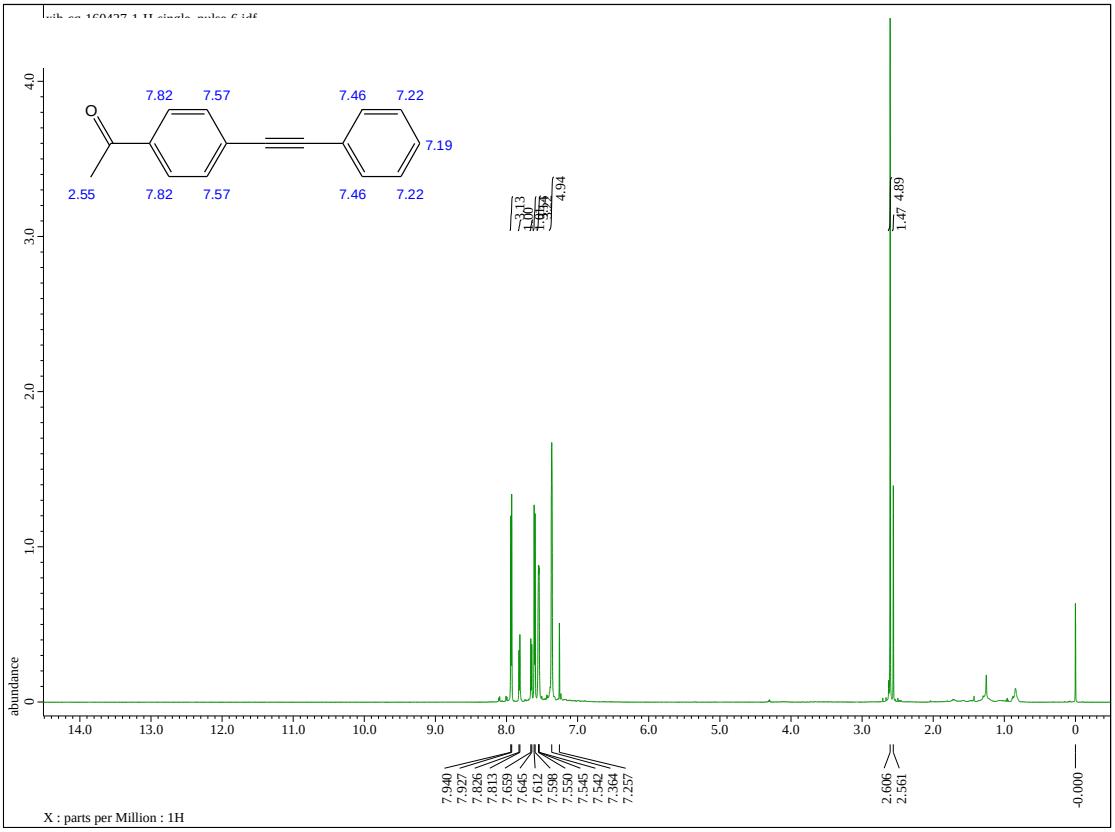

Figure S9. ^{1}H NMR spectrum of the product of Sonogashira coupling reaction between 4-iodoacetophenone and phenylacetylene.

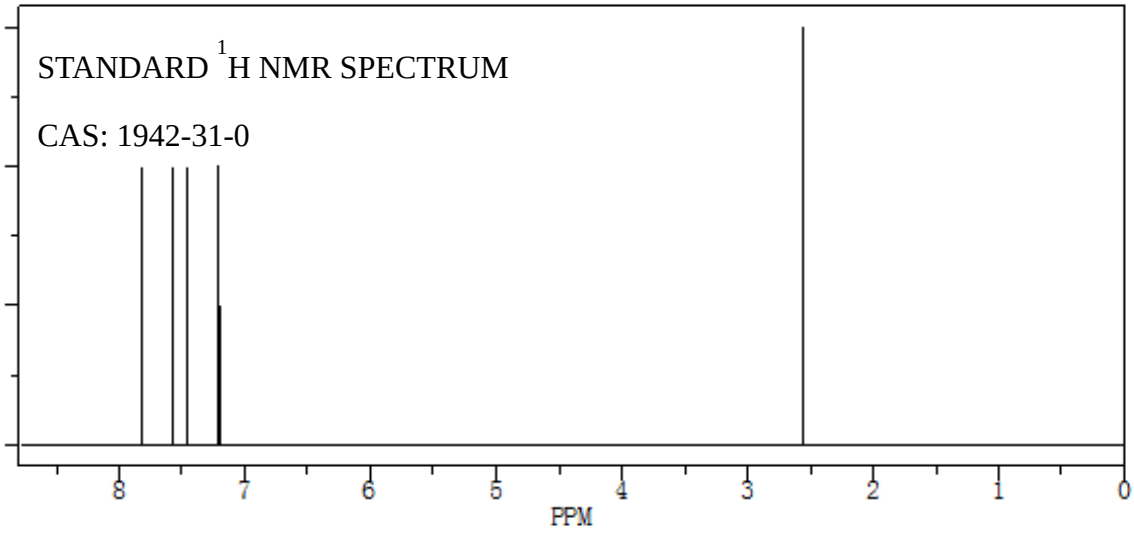

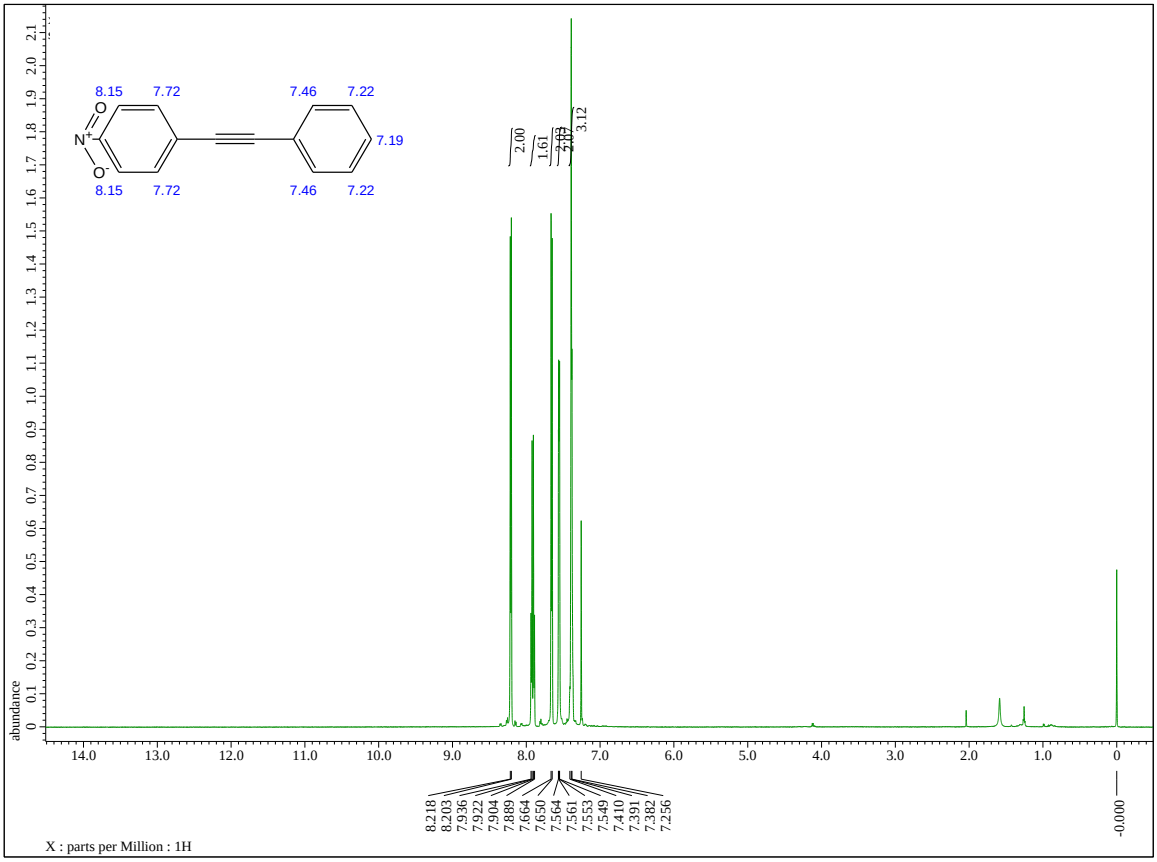

Figure S10. ^{1}H NMR spectrum of the product of Sonogashira coupling reaction between 1-iodo-4-nitrobenzene and phenylacetylene.

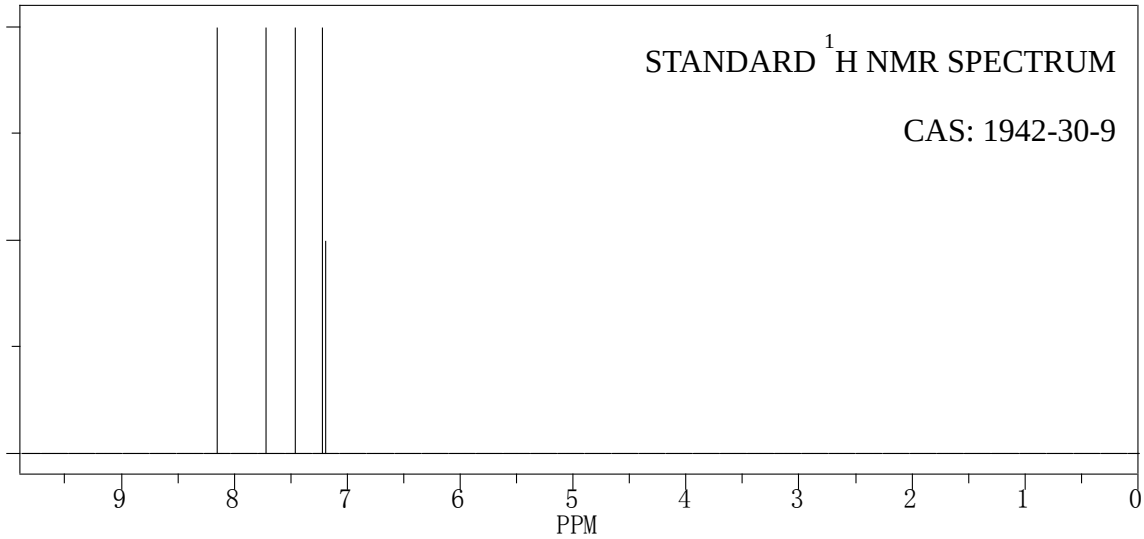

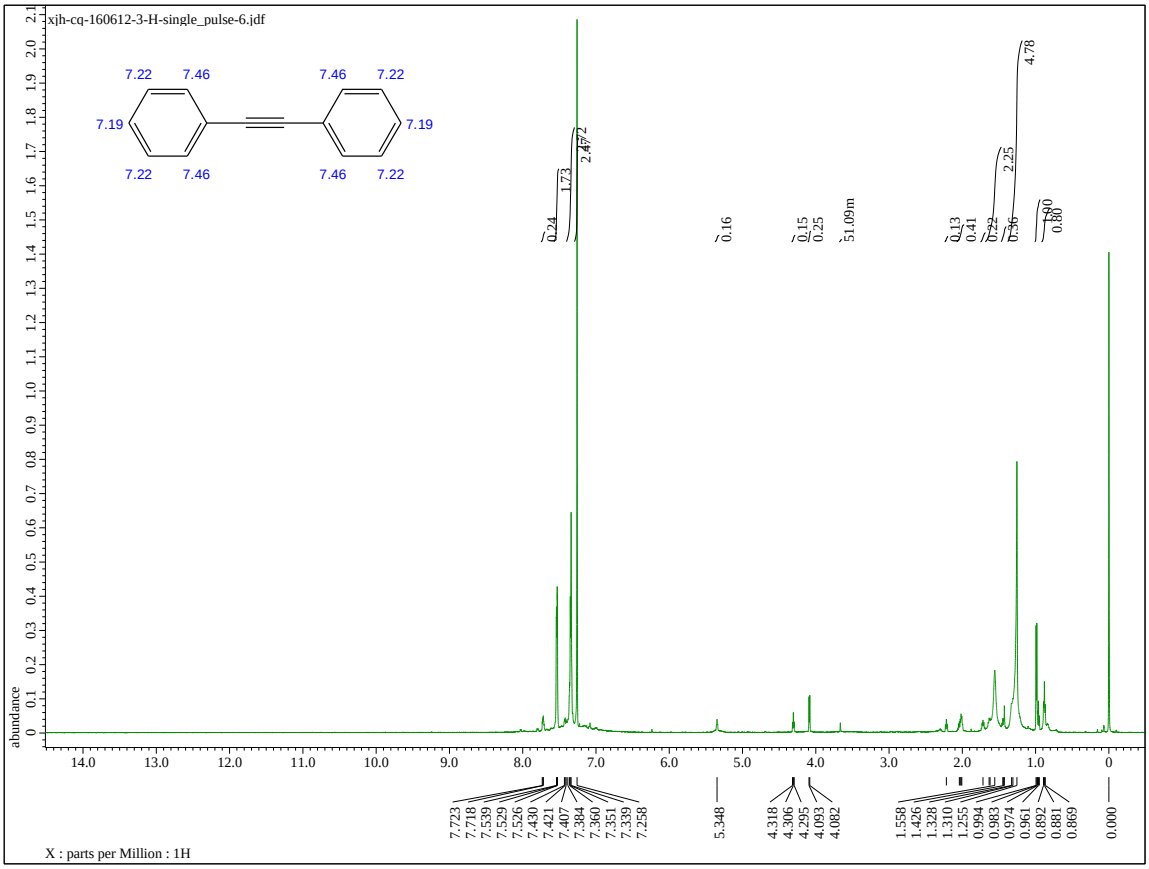

Figure S11. ^{1}H NMR spectrum of the product of Sonogashira coupling reaction between iodobenzene and phenylacetylene.

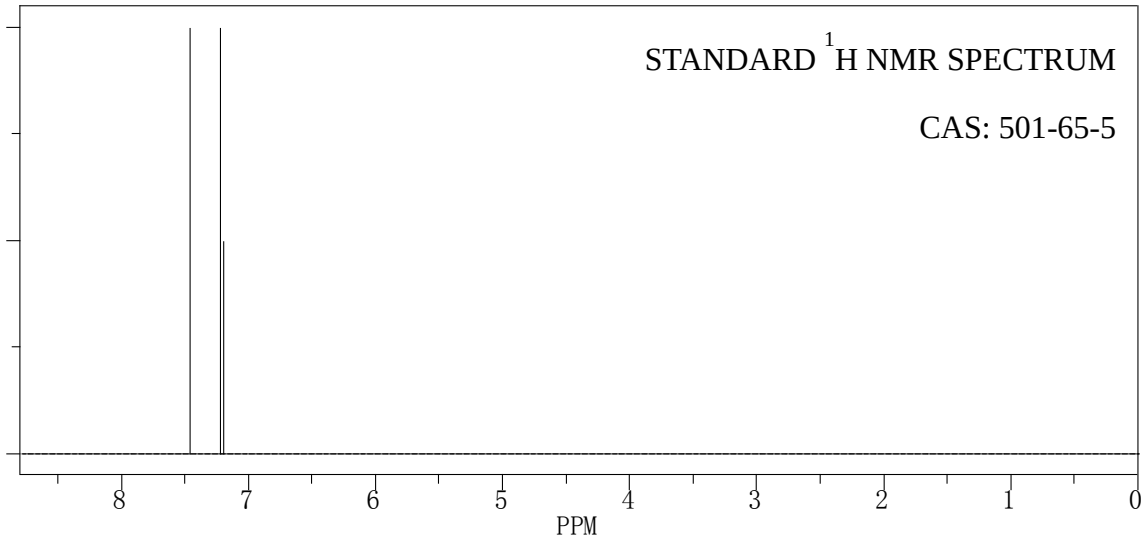

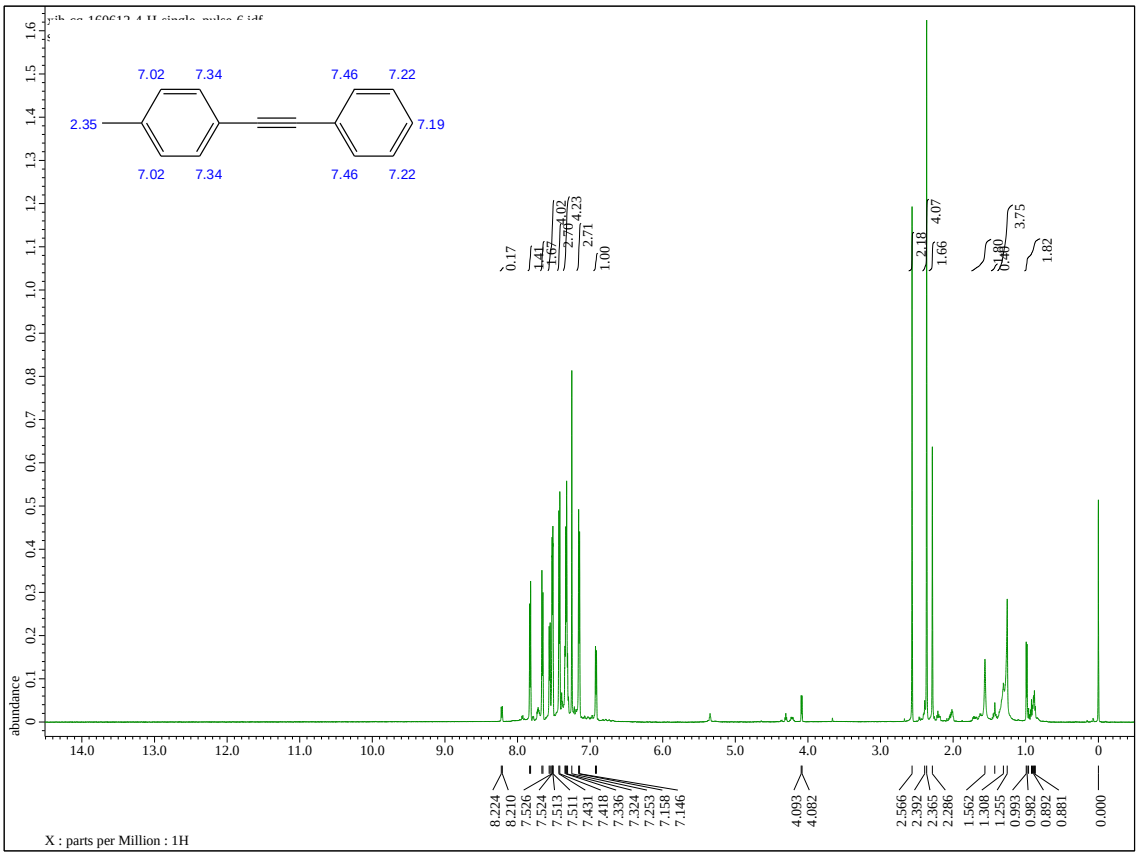

Figure S12. ^{1}H NMR spectrum of the product of Sonogashira coupling reaction between 1-iodo-4-methylbenzene and phenylacetylene.

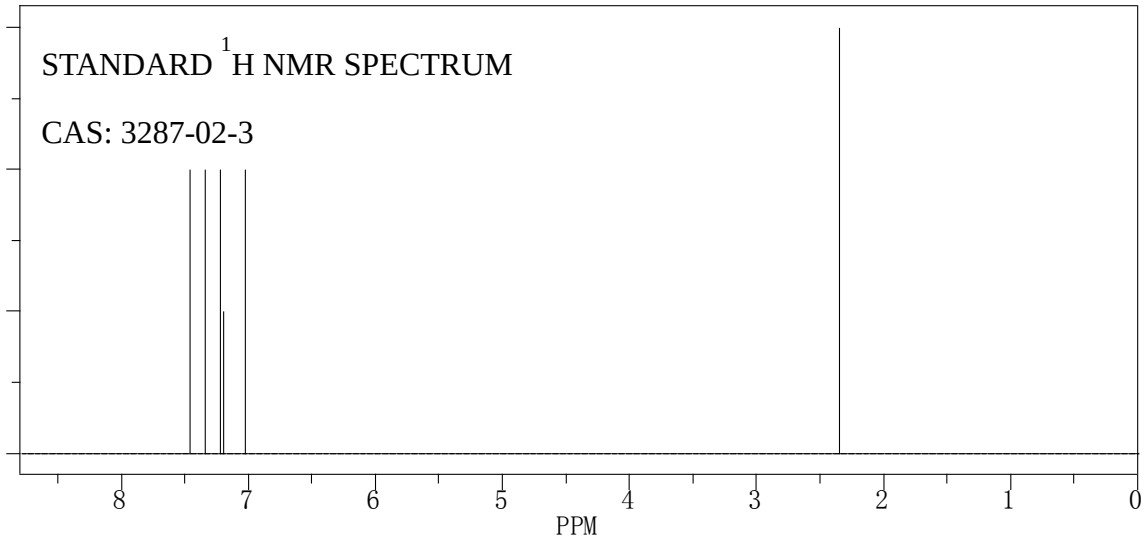

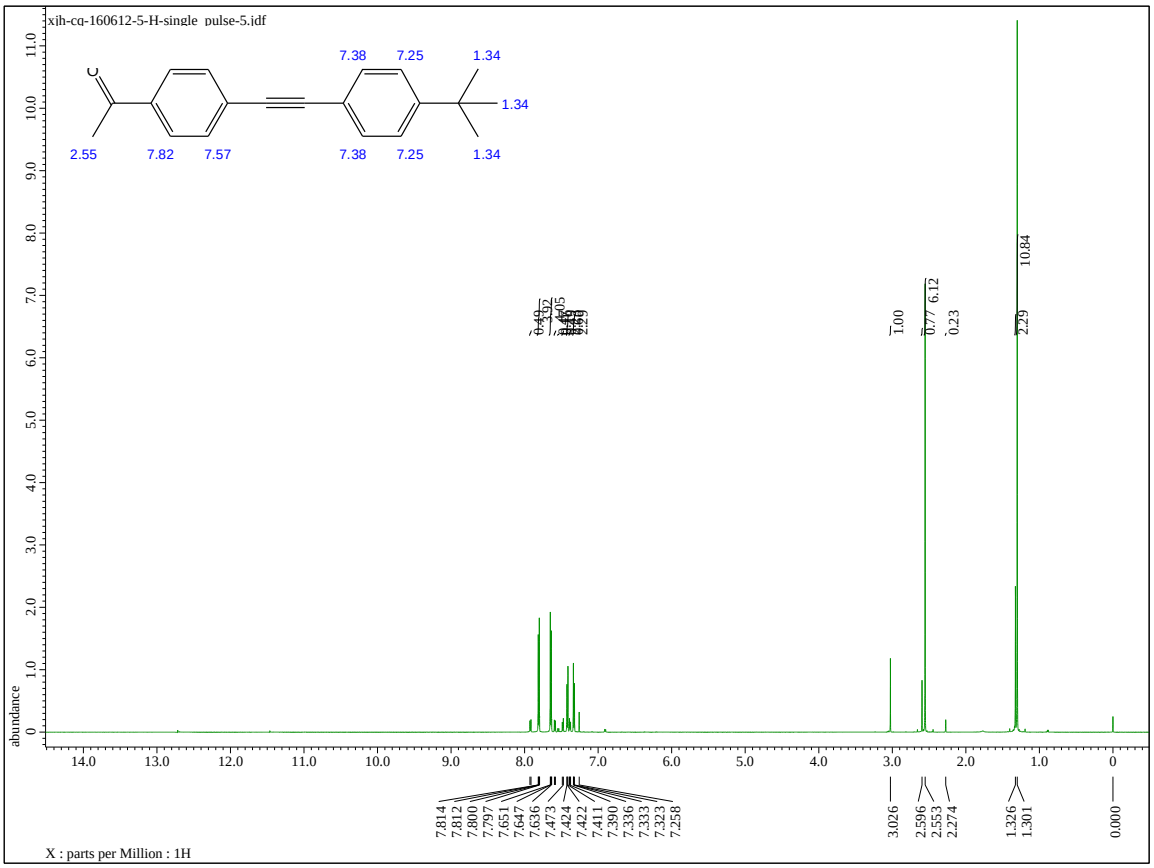

Figure S13. ^{1}H NMR spectrum of the product of Sonogashira coupling reaction between 4-iodoacetophenone and 4- (tert-butyl) phenylacetylene.

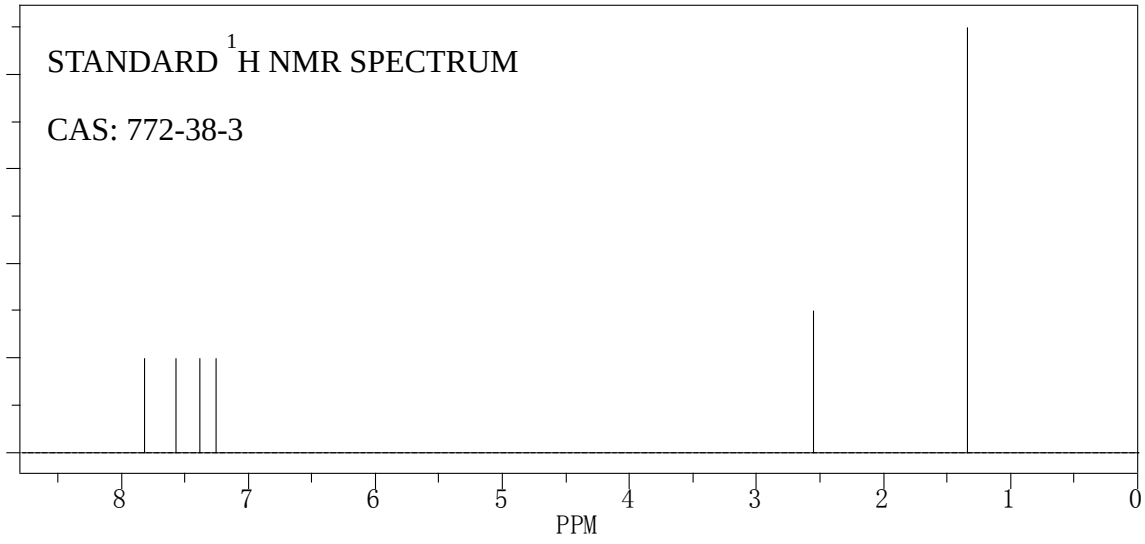

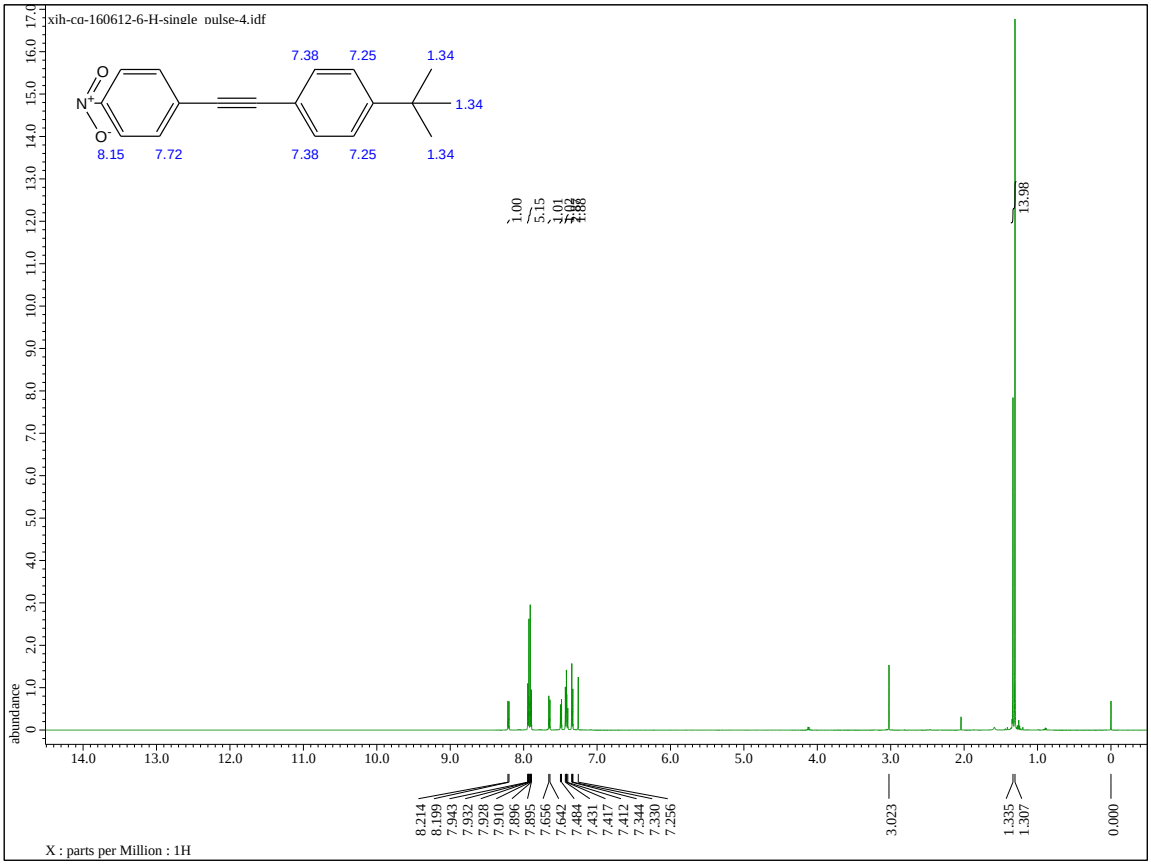

Figure S14. ^{1}H NMR spectrum of the product of Sonogashira coupling reaction between 1-iodo-4-nitrobenzene and 4- (tert-butyl) phenylacetylene.

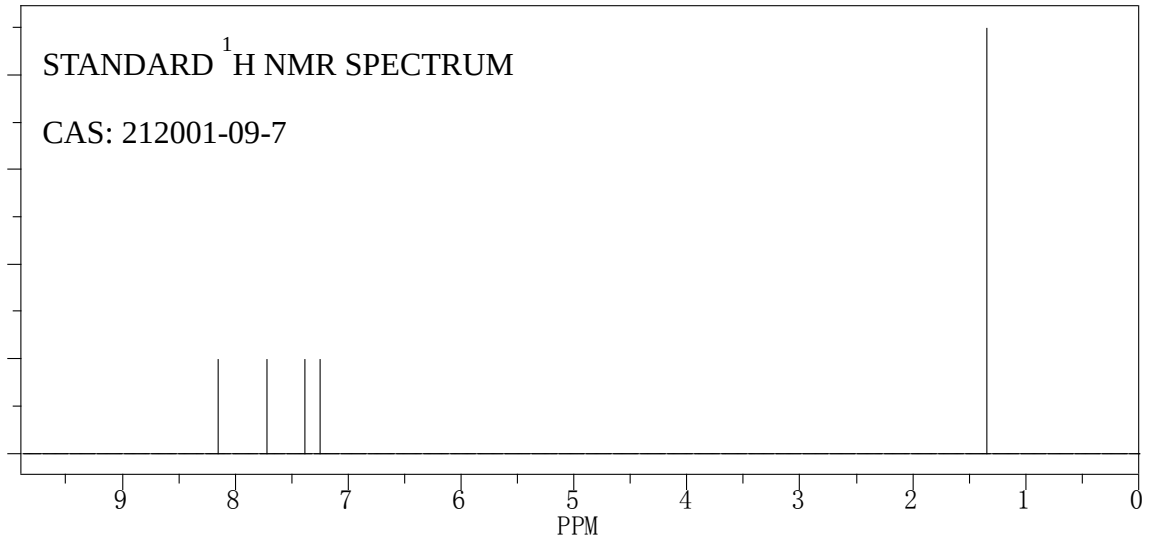

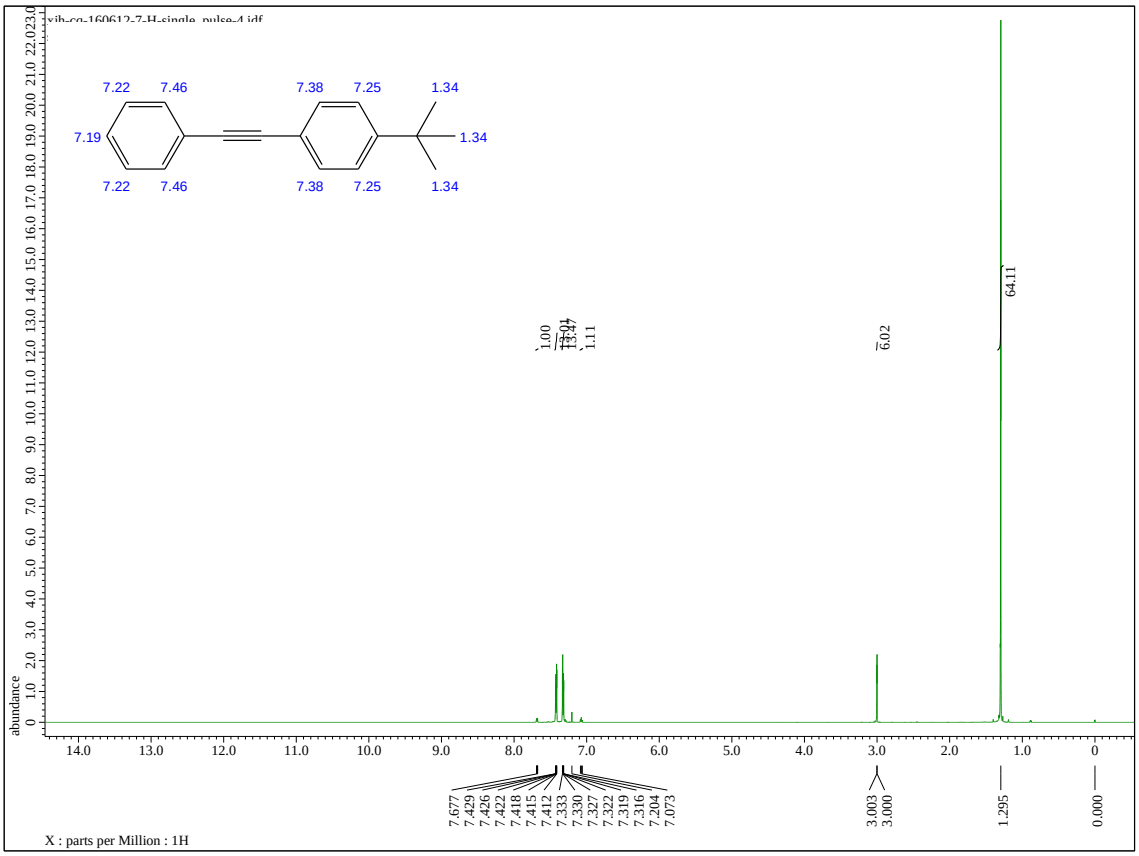

Figure S15. ^{1}H NMR spectrum of the product of Sonogashira coupling reaction between iodobenzene and 4- (tert-butyl) phenylacetylene

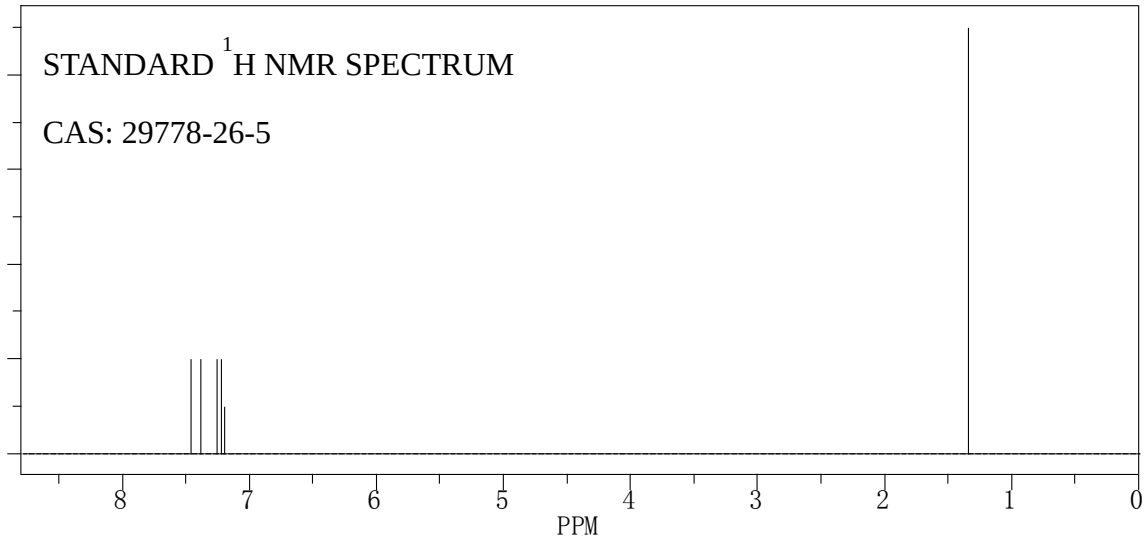

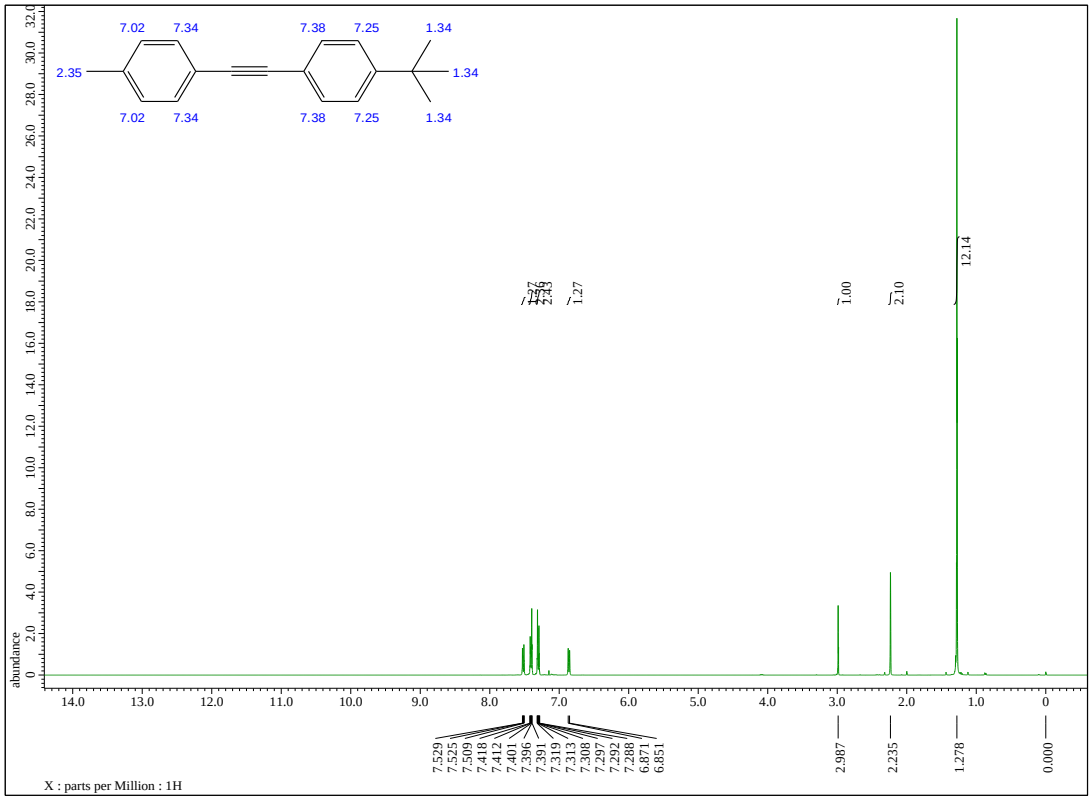

Figure S16. [1]H NMR spectrum of the product of Sonogashira coupling reaction between 1-iodo-4-methylbenzene and 4- (tert-butyl) phenylacetylene.

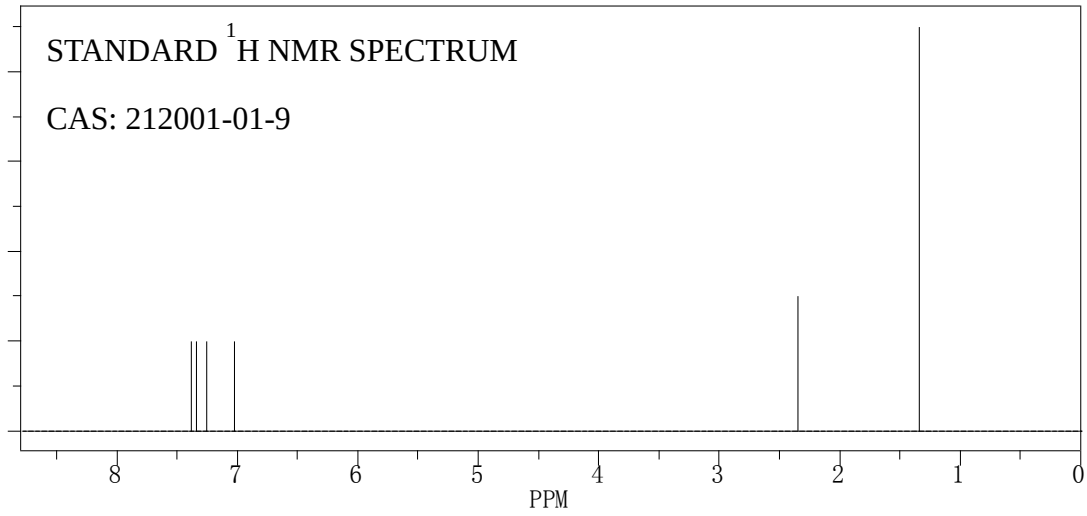

REFERENCES

1 Zhao, H., Xu, J. H., Wang, T., Luo, G. S. A novel microfluidic approach for preparing chi-tosan–silica core–shell hybrid microspheres with controlled structures and their catalytic performance. Lab Chip, 2014, 14, 1901-1906.